Kidney International, Vol. 59 (2001), pp. 1363–1373

Gene expression profile in streptozotocin-induced diabetic mice kidneys undergoing glomerulosclerosis

Jun Wada, Hong Zhang, Yoshinori Tsuchiyama, Keita Hiragushi, Kazuyuki Hida, Kenichi Shikata, Yashpal S. Kanwar, and Hirofumi Makino

Department of Medicine III, Okayama University Medical School, Okayama, Japan; Department of Nephrology, The First Teaching Hospital, Beijing Medical University, Beijing, China; and Department of Pathology, Northwestern University Medical School, Chicago, Illinois, USA

Gene expression profile in streptozotocin-induced diabetic mice kidneys undergoing glomerulosclerosis.

Background. To elucidate the molecular mechanism of diabetic nephropathy, a high-density DNA filter array was employed to survey the gene expression profile of streptozotocin-induced diabetic CD-1 (ICR) mouse kidneys.

Methods. Ten-week-old CD-1 male mice were divided into four groups: (1) control, (2) unilaterally nephrectomized (UX) mice, (3) streptozotocin (STZ)-induced diabetic (STZ) mice, and (4) STZ mice with unilateral renal ablation (STZ-UX). Pathological changes were examined at 24 weeks after the induction. The gene expression profile was compared between the control and STZ mice by a Gene Discovery Array (GDA).

Results. The glomeruli in UX mouse kidney showed prominent glomerular hypertrophy, while the accumulation of mesangial matrix was minimal. Both STZ and STZ + UX mice had significant glomerular hypertrophy and glomerulosclerosis, and the lesions were not enhanced by renal ablation. By comparison between control and STZ mice, 16 clones that increased in expression with the induction of diabetes and 65 clones that decreased in diabetic kidneys were identified. The 37 known genes were related to glucose and lipid metabolism, ion transport, transcription factors, signaling molecules, and extracellular matrix-related molecules. The genes known to be involved in cell differentiation and organogenesis in various tissues (that is, Unc-18 homolog, POU domain transcription factor 2, lunatic fringe gene homolog, fibrous sheath component 1, Sox-17, fibulin 2, and MRJ) were found to be differentially expressed in the early phase of diabetic kidneys.

Conclusions. Hyperglycemia is a major determinant of glomerulosclerosis in STZ-induced diabetic CD-1 mice, and the altered gene expression in the early phase of diabetic kidney may be critical for the development of diabetic nephropathy.

Key words: CD-1 (ICR) mouse, diabetic nephropathy, hyperglycemia, tubulointerstitial fibrosis, end-stage renal failure.

Received for publication June 27, 2000
and in revised form October 23, 2000
Accepted for publication October 26, 2000

© 2001 by the International Society of Nephrology

In types 1 and 2 diabetes mellitus, persistent hyperglycemia induces progressive and irreversible glomerulosclerosis, tubular atrophy, and interstitial fibrosis that ultimately results in end-stage renal failure. Data in a large body of literature point to a number of mechanisms that are involved in the pathogenesis of diabetic nephropathy. They include accumulation of nonenzymatic glycated end products in the kidney, oxidation of renal glycoproteins by reactive oxygen species, intracellular accumulation of sorbitol generated by the reduction of glucose by aldose reductase, activation of the protein kinase C (PKC)-diacylglycerol pathway, and alterations in intrarenal hemodynamics. However, a precise molecular basis for the evolution of renal lesions in diabetes still remains unclear.

In mammalian tissues, mRNA expression, related to the transcriptional activity of various genes, is in a state of dynamic turnover in various developmental and pathophysiological states. In such a process, various genes are differentially up- or down-regulated depending on a given disease process. Currently, exhaustive investigations are being carried out in several laboratories to isolate differentially expressed known or unknown genes in various diseases. The isolation of such genes not only would lead to the identification of candidate disease-susceptible or resistant genes, but also would delineate novel mechanisms and pathways that are involved in various diseases. With that knowledge, potential pharmacological or molecular therapeutic strategies targeted at various steps of a given disease process can be ultimately developed. To identify genes that are differentially expressed in kidneys in a hyperglycemic state or hyperfiltration, we previously utilized representational difference analysis of cDNA (cDNA-RDA) and identified some of the differentially expressed genes [1, 2]. However, by this polymerase chain reaction (PCR)-based subtraction cloning method, that is, cDNA-RDA, it is difficult to establish a comprehensive expression profile of various genes that

can enable one to delineate various biosynthetic or signaling pathways involved in a given disease process or to identify the interrelated genes. Such goals can be achieved only if hundreds or thousands of genes can be simultaneously screened [3].

In view of these considerations, we employed a high-density DNA filter array [Gene Discovery Array (GDA)] to define the transcriptional response to hyperglycemia in the kidney. By this method, approximately 20,000 non-overlapping and nonredundant expressed sequence tag (EST) clones are selected by bioinformatics and plotted on nylon filter to delineate the differential expression by hybridizing filters with radiolabeled cDNA probes derived from control and experimental groups. At present, the GDA is applicable only for the known human and mouse genes and the unknown genes available as EST mouse or human clones in the National Center for Biotechnology Information (NCBI) database; thus, an animal model of mouse with diabetes mellitus was selected.

Our choice of animal model of diabetes, the streptozotocin-induced diabetic ICR mouse [1], was based upon the following considerations. First, with this model, one can study the genes that are relevant to the early phases of diabetes since there is an acute onset of hyperglycemia. Second, in current study, we revealed that the chronic renal lesions of STZ-induced CD-1 mice show a certain degree of mesangial expansion and sclerosis, that is, diffuse lesions, similar to that in human diabetic nephropathy, although marked species or strain differences with respect to the severity of glomerulosclerosis are also noted after the induction of diabetes or subtotal renal ablation [4]. Third, the onset of hyperglycemia associated with spontaneous type 2 diabetes mellitus of mice is insidious, and one cannot negate the influence of hypertension, dyslipidemia, and obesity. Moreover, the lesions in spontaneous models of type 2 diabetes mellitus are distinct from human diabetic nephropathy since they are accompanied with deposition of lipids [5], immune complexes, and amyloid in the renal glomerulus [6].

In this study, the initial experiment was directed to the investigation of pathological alterations of glomeruli of STZ-induced diabetic ICR mice to examine the feasibility of using this mouse strain for the animal model of diabetic nephropathy. In the second step, the changes of gene expression profile in the early phase of diabetes, that is, the hypertrophic phase, were surveyed by high density DNA array.

METHODS

Experimental design

Eighty 10-week-old male ICR mice, Crj: CD-1 (ICR), were obtained from Charles River Co. (Yokohama, Japan) and divided into four groups, each with 20 animals, as follows: control sham operated group, unilaterally nephrectomized mice (UX mice), streptozotocin (STZ)-induced diabetic mice (STZ mice), and STZ-induced diabetic mice with unilateral nephrectomy (STZ-UX mice). Diabetes was induced by an intraperitoneal injection of STZ (200 mg/kg of body weight) in citrate buffer, pH 4.6, and control and UX mice received buffer only. At 2 and 24 weeks after the induction of diabetes, 10 mice from each group at a given time interval were sacrificed, and their kidneys were harvested. The kidneys were processed for morphological studies and total RNA extraction followed by hybridization with high-density DNA filter array.

Morphological studies

The kidneys were fixed in 10% buffered formaldehyde and embedded in paraffin. Three-micrometer thick sections were stained with periodic acid silver methenamine (PAM). The area encompassing the entire glomerulus including sclerotic lesions was measured with image analysis software OPTIMAS version 6.5 (Media Cybernetics, Silver Spring, MD, USA). The cross-section yielding the maximum diameter of the glomerulus was photographed and converted into a digital image, and a total of 50 glomeruli was examined from each animal. In addition, ultrastructural examination of some of the glomeruli was carried out in kidney tissues processed for electron microscopy as previously described [7].

Analyses of gene expression profile by high-density DNA array

A GDA Mouse version 1.1 (Genome Systems, St. Louis, MO, USA) was employed for comparison of the gene expression profiles in control versus STZ mouse kidneys. The cDNA clones spotted on Nylon filter were selected by Genome Systems Inc. using bioinformatics and characterized as follows: from the raw mouse EST (expressed sequence tag) sequences, represented in the I.M.A.G.E libraries, the sequences of the matching vector, bacteria, mitochondria, and ribosomal RNA, and the masking regions with matching repetitive elements, and simple repeats with the ambiguity base code (N) were removed, and that yielded in 207,224 high-quality EST sequences. Of these 207,224 EST clones, clusters of ESTs were generated from pairs that had at least a 95% sequence identity over a minimum 40 bp overlap. This resulted in the grouping of 939 as known full-length clones from the Mouse Gene Index clusters (TIGR; Institute for Genomic Research), 14,154 as clustered representative clones and 4222 as singleton clones. These 19,315 clones, including full-length, clustered, and singleton clones, were spotted on a Nylon filter in duplicate. In addition, 32 *Arbidopsis* and *Drosophila* clones, serving as controls, and 24 orientation markers were spotted.

Total RNA from whole kidney was extracted by the guanidinium isothiocyanate-CsCl ultracentrifugation

method, and mRNA was isolated by oligo-(dT) cellulose chromatography using the FastTrack 2.0 Kit (Invitrogen, San Diego, CA, USA) [8–11]. The mRNA, isolated from various groups, was used for preparing the cDNAs by the Genome Systems as follows: Approximately 2.5 μg of mRNA from normal or diabetic mouse kidneys were used to prepare radiolabeled first-stranded cDNA by employing MMLV (mouse molony leukemia virus) reverse transcriptase (Promega, Madison, Wisconsin, USA), 10 mmol/L dA/dG/dT mix, 10× MMLV buffer and [α-^{33}P]dCTP. As an internal control, run-off RNA corresponding to the *Arbidopsis* and *Drosophila* internal control clones was spotted on GDA filters. The labeled internal control and cDNAs of various control and experimental animal groups were combined, and the total volume was adjusted to 46.5 μL by the addition of sterile water. The unlabeled RNA was degraded by the addition of 12.5 μL of 1 N NaOH and incubating it at 37°C for 10 minutes. The samples were then neutralized by the addition of 12.5 μL Tris buffer, pH 6.8, and 10.0 μL HCl. Degraded RNA and unincorporated nucleotides were removed by G-50 spin column chromatography (Amersham, Arlington Heights, IL, USA). A [α-^{33}P]dCTP-radiolabeled DNA orientation marker, which ensures the correct identification of all the spots on GDA filter, was also prepared with *Rediprime* DNA labeling system (Amersham) and purified as described previously in this article.

Gene Discovery Array filters were prehybridized with 15 mL of prewarmed NothrnMax Hybridization buffer (Ambion, Austin, TX, USA) at 42°C overnight. This was followed by hybridization with labeled control and sample probes in 15 mL of NothrnMax hybridization buffer, containing denatured salmon sperm DNA at 42°C for overnight. Filters were washed twice with 2 × standard saline citrate (SSC) and 1% sodium dodecyl sulfate (SDS) at 68°C for 30 minutes each, followed by another two washes with 0.6 × SSC and 1% SDS at 68°C. The filters were then imaged by a phosphorimager (Molecular Dynamics, Sunnyvale, CA, USA) set at a resolution of 100 microns in a monochromatic mode, and the data were analyzed with Genome Discovery Software (Genome Systems). The density values of neighboring pixels surrounding each four by four-primary square were used as background density. The density data were subtracted from background density.

Clone identification

The Unigene ID and gene name for each EST clone were searched via the updated database at UniGene Mouse Sequence Collection at *http://www.ncbi.nlm.nih.gov/UniGene/Mm.Home.html* (National Library of Medicine; NCBI).

Table 1. Metabolic data after the induction of diabetes and unilateral nephrectomy

	Kidney weight	Body weight	Kidney/body weight %	Plasma glucose
	g			*mg/dL*
2 weeks				
Control	0.34 ± 0.03	36.7 ± 3.9	0.94 ± 0.12	150.2 ± 25.3
UX	0.45 ± 0.07	36.2 ± 3.1	1.25 ± 0.26	136.3 ± 24.0
TZ	0.42 ± 0.10	34.8 ± 2.0	1.21 ± 0.28	555.4 ± 51.39[b]
STZ-UX	0.54 ± 0.19	35.7 ± 4.0	1.53 ± 0.58	542.1 ± 46.2[b]
24 weeks				
Control	0.39 ± 0.03	50.0 ± 0.8	0.78 ± 0.07	110.3 ± 5.3
UX	1.53 ± 0.08[a]	46.0 ± 2.2	3.34 ± 0.14[b]	105.8 ± 7.9
STZ	0.58 ± 0.18	42.0 ± 6.7[a]	1.36 ± 0.25	454.0 ± 196.2[b]
STZ-UX	0.81 ± 0.26	41.3 ± 8.0[a]	2.02 ± 1.02	392.2 ± 205.9[b]

Abbreviations are: UX, unilaterally nephrectomized ICR mice; STZ, streptozotocin (STZ)-induced diabetic ICR mice; STZ-UX, STZ-induced diabetic ICR mice with unilateral nephrectomy.

[a] $P < 0.05$ vs. control ICR mice; [b] $P < 0.01$ vs. control ICR mice

Statistical analysis

The data are expressed as mean ± SD, and a P value of less than 0.05 was determined by Student t test.

RESULTS

Metabolic and morphological studies

In STZ and STZ-UX mice, sustained hyperglycemia was observed throughout the entire period of 24 weeks, and body weights were significantly reduced (Table 1). The kidney weight and kidney/body weight ratio were significantly increased in UX and UX-STZ mice compared with the control. The UX mice had hypertrophied glomeruli; however, the matrix accumulation in the mesangium was minimal. In contrast, STZ and STZ-UX revealed marked glomerular hypertrophy and an increase in the mesangial matrix (Fig. 1). Some of the glomeruli had undergone segmental sclerosis as well. The morphometric analyses indicated that the glomerular size was significantly increased in UX, STZ, and STZ-UX mice, and the mesangial area was significantly expanded in STZ and STZ-UX mice (Fig. 2). The unilateral renal ablation did not contribute to any significant increase in the glomerular volume or mesangial expansion in STZ mice. Ultrastructural examination did not reveal the presence of any electron dense or amyloid and lipid deposits in the glomeruli of STZ mice kidneys. However, expanded mesangial area with some reduction in the capillary filtration surfaces were observed (Fig. 3).

Gene expression profile in normal mouse kidneys

The GDA filters hybridized with radiolabeled control and STZ mouse kidney cDNAs are shown in Figure 4. Although the background hybridization signals were similar in both normal and STZ filters, a certain "blooming" action of positive hybridization signals into adjacent

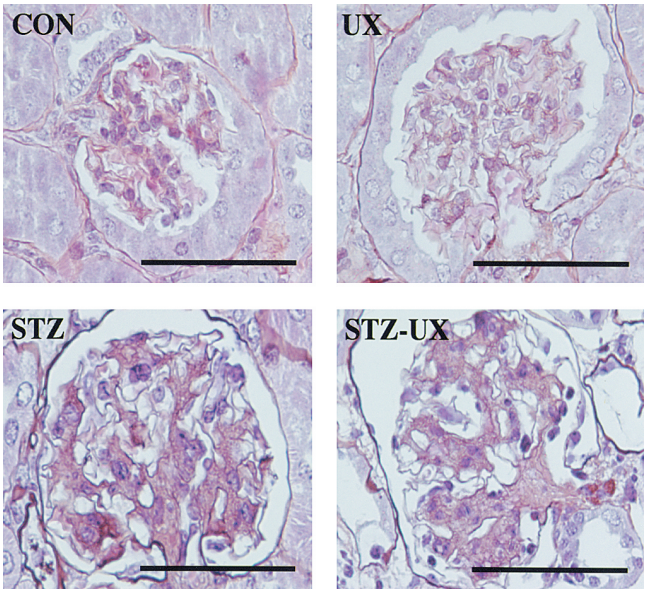

Fig. 1. Light micrographs of glomeruli of ICR mice kidney. The glomeruli in unilaterally nephrectomized mouse (UX) show prominent glomerular hypertrophy and minimal accumulation of mesangial matrix. In contrast, streptozotocin (STZ)-induced diabetic ICR mouse (STZ) and STZ mouse with unilateral nephrectomy (STZ-UX) reveal significant glomerular hypertrophy, a marked increase in the mesangial matrix. (PAM, periodic acid silver methenamine stain; bar = 50 μm).

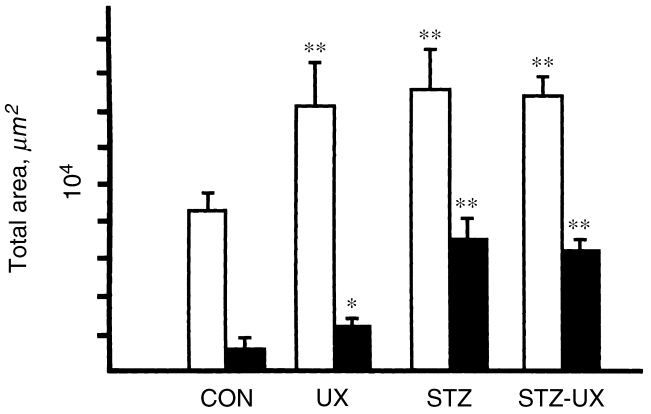

Fig. 2. Morphometric analyzes of glomeruli of mice kidney. Area of the glomerulus and mesangium are measured with image analysis software OPTIMAS version 6.5. The glomerular size is increased in UX, STZ, and STZ-UX mice, while mesangial matrix only in STZ and STZ-UX mice compared with the controls. Abbreviations are: CON, control ICR mice; UX, unilaterally nephrectomized mice; STZ, streptozotocin (STZ)-induced diabetic mice; STZ-UX, STZ-induced diabetic mice with UX.

wells was observed. Using Genome Discovery Software, EST clones were selected by their average intensity of two spots. The number of the identified clones in normal and diabetic mouse kidneys was defined according to various intensity thresholds (Table 2). By setting a minimal intensity threshold at 2000, approximately 1008 and 829 clones were identified in normal and diabetic kidneys, respectively. The top 50 highly expressed genes in normal kidney are indicated in Table 3. Kidney androgen-regulated protein was ranked at the top, and apparently, it is the most abundant transcript in mouse proximal tubules [12]. By searching the UniGene database, 50 genes were classified under three categories as follows: known mouse genes ($N = 25$), orthologs corresponding to rat and/or human known genes ($N = 8$), and unknown single EST or clustered ESTs ($N = 17$). The latter category indicates that approximately one third of the abundantly expressed transcripts were novel genes.

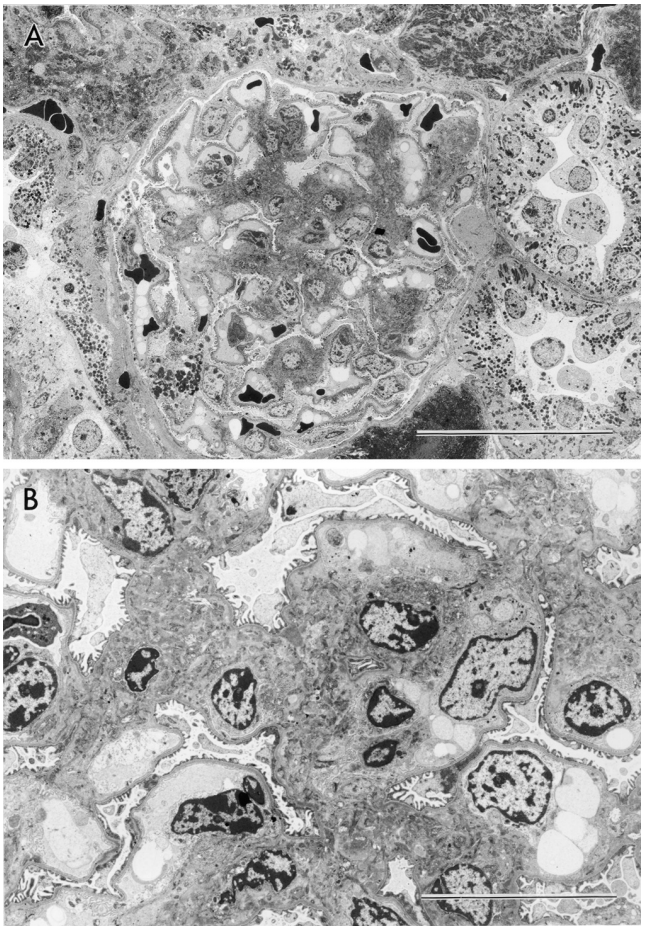

Fig. 3. Low (*A*) and high (*B*) magnification electron micrographs of the glomerulus from STZ-induced diabetic mouse. An expansion of the mesangial matrix and the narrowing of capillary lumens, similar to human diabetic nephropathy, is observed. (A, bar = 50 μm; B, bar = 20 μm).

Comparison of gene expression profiles between normal versus diabetic kidneys

Since detection of less abundantly expressed genes with a lower spot intensity would be readily influenced by the [α-^{33}P]dCTP hybridization background, there is a good chance of isolating false positive clones that do not have any differential expression. Thus, the EST clones

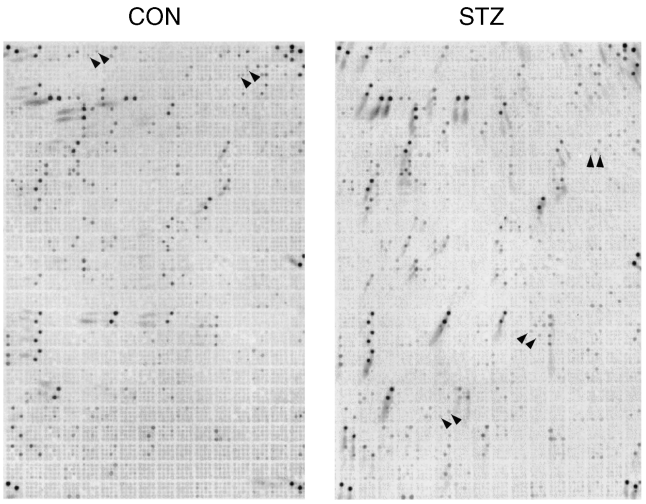

Fig. 4. Comparison of gene expression profile of control and streptozotocin (STZ)-induced diabetic kidney by high-density DNA array. The mRNA of control and STZ mouse kidneys was extracted, radiolabeled with [α-^{33}P]dCTP, and hybridized with Gene Discovery Array (GDA) Mouse version 1.1. About one sixth of the total filter area of control (CON) and STZ-induced diabetic (STZ) kidneys is shown. In each corner, the intense hybridization spots of DNA orientation markers are observed. All clones are double spotted to negate the false hybridization signals or high background. The genes with a spot to spot ratio greater than five was selected by Genome Discovery Software. Since the "blooming" action of positive hybridization signals into adjacent wells is observed, spots of the screened genes are visually inspected.

with an average intensity of more than 2000 in normal and/or diabetic kidneys were analyzed. Approximately 1008 clones in normal and 829 clones in diabetic kidneys were selected (Table 2). To ensure the specificity, any spot with a spot–to–spot ratio of greater than five was considered as significantly and differentially expressed. In addition, spots of the screened genes were visually inspected since the "blooming" action of positive hybridization signals into adjacent wells was observed. Analyses by Genome Discovery Software revealed that 16 clones had increased expression with the induction of diabetes and 65 clones had decreased expression in the diabetic kidneys. According to the mouse Unigene database at the NCBI, the differentially expressed genes could be classified into four groups: known mouse genes ($N = 31$); orthologous genes corresponding to rat and/or human known genes ($N = 6$); homologous genes with moderate to weak similarity to yeast, nematodes, and mammalian genes ($N = 5$), and unknown single EST or clustered ESTs ($N = 39$). Thus, 44 ESTs out of 81 identified clones were novel genes. Finally, the genes were also classified into five categories according to their biological functions. These included those related to the biosynthesis and degradation of lipids and amino acids ($N = 7$), ion transport, biosynthetic precursors and organelles ($N = 6$), transcription and protein synthesis ($N = 8$), signaling ($N = 3$), and extracellular matrix (ECM) molecules ($N = 2$), and 15 genes were related to cell differentiation, proliferation, and survival (Table 4).

Table 2. Comparison of the renal gene expression profile between control and streptozotocin (STZ)-induced diabetic ICR mice

	Intensity thresholds				
	1000	2000	3000	4000	5000
Control[a]	2460	1008	676	502	413
STZ[a]	1407	829	561	438	371
STZ > Control[b]	60	16	5	4	3
STZ < Control[c]	647	65	18	11	5

[a] The number of genes filtered with various minimum intensity thresholds in control and STZ mice is shown.
[b] The number of up-regulated genes in STZ-induced diabetic mice with a spot-to-spot ratio greater than five is indicated; they are also filtered with various intensity thresholds.
[c] The number of down-regulated genes in STZ-induced diabetic mice with a spot-to-spot ratio greater than five is shown; they are also filtered with various intensity thresholds.

DISCUSSION

The data of this investigation suggest that in the STZ-induced diabetic ICR mouse kidney, hyperglycemia had the major role in the development of mesangial lesions progressing to glomerulosclerosis, and unilateral renal ablation only contributed minimally to the accentuation of the disease process. In addition, the data from the High Density DNA Array provided a global assessment of alterations of the gene expression in the kidney during the early phases of STZ-induced diabetes that preceded glomerulosclerosis, although expression profile was related to not only transcriptional activities but also RNA stability and post-transcriptional factors, which contributed to a certain degree of the observed difference in RNA amount. It was anticipated that individual analyses of these genes, as discussed later in this article, may enhance our understanding of the events or the processes involved in the pathogenesis of diabetic nephropathy.

Genes relevant to glucose and lipid metabolism

Liver is the primary site of glucose production. However, recent studies utilizing isotopic and balance techniques suggest that approximately 25% of the systemic glucose is produced in the kidney via gluconeogenesis from precursors such as lactate, glutamine, and glycerol [13, 14]. Conceivably, the kidney is an important source of glucose production in STZ-induced diabetic rats [15] and human type 2 diabetes [14, 16]. Although enzymes related to gluconeogenesis were not found in this investigation, one of the genes involved in carbohydrate metabolism, for example, glucagon receptor, was found to be differentially expressed. Glucagon receptor is normally expressed in liver, pancreatic β cells, kidney, and adipose tissue [17]. Its precise biological role in most of the tissues

Table 3. Abundantly expressed genes in control kidney of male ICR mice

GenBank ID	Unigene ID	Intensity	Gene name
AA116857	Mm.13052	107581.55	Kidney androgen-regulated protein
AA278096	Mm.21961	54801.82	ESTs, highly similar to C7–1 protein [R. norvegicus] (93%/196)
AA172974	Mm.28050	49691.93	ESTs, highly similar to CD2 cytoplasmic domain-binding protein [H. sapiens] (91%/164 aa)
AA445684	Mm.20418	42679.32	Solute carrier family 17 (sodium/hydrogen exchanger), member 2
AA170738	Mm.25125	36367.28	ESTs, highly similar to ribose-phosphate pyrophophokinase [R. norvegicus] (99%/145 aa)
AA512768	Mm.5291	36269.04	Ribosomal protein S5
AA444364	Mm.19367	33746.57	ESTs, highly similar to myosin light chain 1, slow twitch muscle B/ventricular isoform [R. norvegicus] (95%/156 aa)
AA445571	Mm.35779	33182.43	ESTs, highly similar to TFIIIC2 subunit [H. sapiens] (91%/166 aa)
AA509386	Mm.18300	32547.15	NBAT (neutral and basic amino acid transporter)
AA123180	Mm.278	32529.72	Uroguanylin
AA469579	Mm.22024	32522.29	Cortactin
AA543556	Mm.4372	31110.81	RAR-related orphan receptor γ
AA124856	Mm.10154	30779.41	Testis-specific protein kinase 1
AA419867	Mm.29617	30653	ESTs, highly similar to protein phosphate inhibitor 2 [R. norvegicus] (92%/168 aa)
AA471833	Mm.9307	29516.27	Transketolase
AA510720	Mm.5274	29356.93	Cu/Zn-superoxide dismutase
AA451352	Mm.4708	27754.28	Tyrosine-protein kinase SYK
AA289387	Mm.29768	27744.19	Pyruvate dehydrogenase kinase
AA388600	Mm.9745	27366.17	Lactate dehydrogenase 2, B chain
W33527	Mm.18517	25994.99	GTPase-activating protein GAPIII
AA416215	Mm.40186	25990.88	ESTs
AA509502	Mm.40775	25873.03	ESTs, highly similar to GDP-mannose pyrophosphorylase B [H. sapiens] (97%/147 aa)
AA389271	NA	25703.28	EST
AA445597	NA	25595.79	EST
AA388565	NA	25463.97	EST
AA512729	Mm.3373	25407.03	Cofilin, muscle isoform
AA511391	Mm.5265	25328.92	ESTs
AA275948	Mm.37214	25269.73	Perinuclear binding protein PICK1
AA390096	Mm.2632	25216.49	Latexin
AA445523	NA	25214.85	EST
AA432762	Mm.4113	25060.15	ESTs, highly similar to mRNA-associated protein mRNP41 [H. sapiens] (97%/145 aa)
AA475488	NA	24889.7	EST
AA153676	Mm.24007	24781	ESTs
AA511719	NA	24677.37	EST
AA105569	Mm.1408	24462.59	Adrenomedullin
AA396117	Mm.3460	24421.49	CD14 antigen
AA466427	Mm.20927	24180.42	Transforming growth factor beta 1-induced transcript 4
AA518419	Mm.41272	24044.34	ESTs
AA124334	NA	23865.21	EST
AA499913	Mm.29064	23750.2	Cytochrome P450, 2d9
AA124048	NA	23710.51	EST
AA466044	Mm.41348	23640.8	ESTs
AA290108	Mm.29332	23528.61	ESTs
AA500156	Mm.18590	23476.23	Cell surface glycoprotein A15
AA546728	Mm.24156	23407.62	ESTs, weakly similar to cytohesin 2 [M. musculus] (31%/137 aa)
AA396395	NA	23226.02	EST
AA396595	Mm.14868	23069.41	Granzyme G
AA536770	Mm.39990	23047.83	ESTs
AA445222	Mm.9221	23026.03	RAB4A, member RAS oncogene family
AA288222	Mm.3182	22958.49	Interferon consensus sequence-binding protein

is unknown; however, circulatory glucagon may play a role in the regulation of intrarenal hemodynamics in type 1 diabetes mellitus in humans with subsequent effects on the mesangial cell biology [18].

Besides carbohydrate metabolism, several enzymes related to lipid metabolism showed a differential expression in the STZ-induced diabetic mouse kidney. One of the enzymes with up-regulated expression was AMP-activated protein kinase (AMPK), a member of a metabolite-sensing protein kinase family that is regulated by vigorous exercise, nutrient starvation, and ischemia/hypoxia. It modulates cell metabolism by phosphorylating the key enzymes, and as a result, there is a stimulation of hepatic fatty acid oxidation and ketogenesis, inhibition of cholesterol and triglyceride synthesis, lipogenesis and adipocyte lipolysis and stimulation of skeletal muscle

Table 4. Differentially expressed known genes in control and streptozotocin (STZ)-induced diabetic ICR mice

GenBank ID	Unigene ID	Gene name	Function	Intensity of control ICR mice	Intensity of STZ-induced diabetic ICR mice	Intensity ratio
AA238606	Mm.12155	Unc-18 homolog	[b] Vesicle transport and development of kidney	125.53	2293.81	↑ 18.2728
AA445681	Mm.37811	POU domain, class 2, transcription factor 2	[c] Transcription factor that specifically binds the octamer motif, B cell differentiation	465.94	5725.26	↑ 12.2875
AA145856	Mm.1129	40S ribosomal protein S2	[c] Protein synthesis	265.97	2673.17	↑ 10.0507
AA473546	Mm.1319	Glucagon receptor	[a] Glucagon receptor	973.57	6113.16	↑ 6.2791
AA450800	Mm.12834	Lunatic fringe gene homolog	[d] Notch signaling pathway, boundary formation and anterior-posterior somite identity	697.68	4326.08	↑ 6.2006
AA198401	Mm.6670	AMP-activated protein kinase	[a] Metabolic stress-sensing protein kinase by depletion of ATP; inhibition of fatty acid and cholesterol synthesis	624.77	3726.16	↑ 5.9641
AA470164	Mm.23876	ESTs, highly similar to α-propionyl-CoA carboxylase [Rattus norvegicus] (97%/137 aa)	Key enzyme in the catabolic pathway of odd-chain fatty acids, isoleucine, threonine, methionine and valine	958.35	5456.18	↑ 5.6933
AA199215	Mm.5045	Monocarboxylate transporter 2	[b] Monocarboxylate transporter	2043.94	0	↓ > 100
AA215064	Mm.2288	Inter-α-trypsin inhibitor H2 chain	[e] Regulation of localization, synthesis, and degradation of hyaluronan	2069.74	0	↓ > 100
AA033344	Mm.4168	Bumetanide-sensitive Na-(K)-Cl cotransporter 1	[b] Sodium and chloride reabsorption	2128.03	0	↓ > 100
AA106031	Mm.1498	Fibrous sheath component 1	[f] Major structural component of sperm fibrous sheath, spermatogenesis	2014.5	0	↓ > 100
AA107796	Mm.9020	Lectin λ	[f] Macrophage mannose receptor type C lectin	3186.7	51.06	↓ 62.4059
AA003262	Mm.7964	Cartilage-derived retinoic acid-sensitive protein/melanoma inhibitory activity protein	[f] Growth inhibition on melanoma cells and other neuroectodermal tumors	3332.53	65.1	↓ 51.1947
AA466030	Mm.25492	ESTs, highly similar to LCAT-like lysophospholipase [H. sapiens] (91%/35 aa)	[a] Lysophospholipase	6325	316.05	↓ 20.0128
W56965	Mm.28814	Caspase 7	[f] Apoptosis	3504.03	194.58	↓ 18.0081
AA208865	Mm.3776	Perforin 1	[f] Cell lysis	2173.88	126.77	↓ 17.1479
AA004099	Mm.20914	Mitogen- and stress-activated protein kinase-2	[d] Growth-factor and stress-induced activation of CREB	2048.47	123.49	↓ 16.5886
AA286605	Mm.22547	ESTs, highly similar to acid ceramidase [M.musculus] (100%/151 aa)	[a] Hydrolysis of ceramide into shpingosine and free fatty acid	3440.04	234.04	↓ 14.6983
AA212907	Mm.10964	RD PROTEIN	[f] Unknown (possible RNA binding protein)	2171.02	154.56	↓ 14.0465
AA218316	Mm.42201	Hus1-like protein (Hus1)	[f] Mammalian homolog of cell cycle checkpoint gene Hus1	2954.33	261.95	↓ 11.2781

(continued)

Table 4. continued

GenBank ID	Unigene ID	Gene name	Function	Intensity of control ICR mice	Intensity of STZ-induced diabetic ICR mice	Intensity ratio
AA242262	Mm.24870	ESTs, highly similar to ubiquitin carboxyl-terminal hydrolase 7 [H. sapiens] (98%/162 aa)	[c] Protein turnover	2429.66	233.86	↓ 10.3894
AA510115	Mm.19788	BTEB-1 (basic transcription element binding protein 1) transcription factor	[c] Transcription factor that binds to GC box promotor elements	2010.58	205.23	↓ 9.7968
AA238435	Mm.37210	γ-adaptin	[b] Component of the adaptor complexes that link clathrin and to receptors in coated vesicle	2097.53	215.95	↓ 9.7129
AA389102	Mm.4533	Apolipoprotein A-IV	[a] Major component of HDL and chylomicrons	2431.01	257.5	↓ 9.4407
AA041971	Mm.4593	UDP-galactose transporter related isozyme 1	[b] Nucleotide-sugar transporter	4098.04	515.32	↓ 7.9525
AA014729	Mm.5080	Transcription factor SOX-17	[c] Transcriptional activator in the premitotic germ cells	2618.35	349.39	↓ 7.494
W99833	Mm.41650	ESTs, highly similar to RNA-binding protein staufen [M.musculus] (100%/57 aa)	[c] mRNA transport to the rough endoplasmic reticulum	2651.44	362.76	↓ 7.309
W46087	Mm.10230	ATP-dependent RNA helicase A (dead box protein 9)	Regulation of RNA-binding proteins	2028.03	305.85	↓ 6.6308
AA423007	Mm.3871	Phosphatidylserine synthase-2	[a] Phosphatidylserine synthesis	14830.23	2411.89	↓ 6.1488
AA395996	Mm.32920	ESTs, moderately similar to CGI-76 protein [H. sapiens] (83%/99 aa)		2185.34	367.11	↓ 5.9529
AA015261	Mm.9122	Paraoxonase 3	[f] Hydrolyzation of the organophosphorus substrates	2082.5	351.29	↓ 5.9282
W44105	Mm.4609	ESTs, Highly similar to peroxisomal membrane anchor protein [R.norvegicus] (96%/162 aa)	[f] Integral membrane protein of peroxisomes	7165.06	1242.35	↓ 5.7674
W53877	Mm.6120	Fibulin 2	[e] Extracellular matrix, epithelial–mesenchymal interactions	2453.75	442.46	↓ 5.5457
AA189814	Mm.2701	MRJ (mammalian relative of DnaJ)	[f] Development of placenta	2278.55	416.99	↓ 5.4643
AA286651	Mm.22530	EXO70 protein	[b] Exocytosis	2123.43	390.06	↓ 5.4438
AA123156	Mm.24122	ESTs, highly similar to myc far upstream element-binding protein [H. sapiens] (97%/132 aa)	[c] Transcriptional regulation of *c-myc*	2345.44	443.19	↓ 5.2922
AA289799	Mm.14487	MAP kinase kinase 6c	[d] Signal transduction	3259.68	616.72	↓ 5.2855

[a] Lipid glucose and amino acids metabolism
[b] Transporters of ions and biosynthetic precursors and organella
[c] Transcriptional regulation and protein synthesis
[d] Signaling molecules
[e] Extracellular matrix-related molecules
[f] Development, differentiation, survival, and proliferation of the cells

fatty acid oxidation and glucose uptake [19]. Since the AMPK yeast homolog Snf1p plays a major role in adapting to glucose deprivation [20] and AMPK is induced by nutrient starvation in mammalian liver, the up-regulated expression of AMP-activated kinase in diabetic kidney may be a unique tissue-specific response. The other enzymes or associated proteins related to lipid metabolism, that is, α-propionyl-CoA carboxylase, LCAT-like lysopoholipase, and apolipoprotein A-IV, also showed a differential expression. Since dyslipidemia accelerates the progression of glomerulosclerosis in diabetic nephropathy [21–23], it is likely that the alterations in local lipid metabolism in the diabetic kidney may be related to the progression of diabetic nephropathy.

Genes relevant to protein synthesis and transcriptional regulation

In liver, adipose tissue, and muscle, the metabolic alterations induced by diabetes are characterized by an accentuated catabolic response and diminished anabolic activity related to protein and glucose metabolism [24]. In contrast, the anabolic response is accompanied with an increase in RNA [25, 26] and protein synthesis and decreased protein degradation [27], which ultimately leads to renal growth and hypertrophy. Since 40S ribosomal protein S2 and ubiquitin carboxyl-terminal hydrolase 7 are involved in protein synthesis and ubiquitin-mediated protein degradation [28], the increased expression of the former and decreased expression of the latter in this investigation seems to reflect an anabolic response in the diabetic kidney. These observations are in line with the findings reported in previous metabolic studies [24, 25, 27]. Nevertheless, the up-regulated expression of Oct2 (octamer motif-binding transcription factor) [29] and decreased expression of BTEB-1 (GC box-binding transcription factor) [30], Sox-17 [31], and myc-far upstream element binding protein [32] suggest that high glucose or insulin deficiency-induced alterations in the transcriptional regulation are of a rather complex nature. One can expect up-regulation of early response genes, such as *c-fos*, *c-jun*, *c-myc*, which regulate gene transcription and contribute to renal hypertrophy in STZ-induced mouse. They were indeed up-regulated in the rapid phase of STZ-induced diabetic rats 24 hours after the onset of hyperglycemia and returned to baseline by 48 hours [33]. In our experiment, we isolated mRNA two weeks after the induction; thus, the differential expression of these early response genes was not observed.

The alterations in the transcriptional regulation were further reflected in the genes related to mRNA stability and mRNA transport. Staufen is a RNA-binding protein that is localized to the endoplasmic reticulum and is believed to play a role in targeting RNA to its site of translation [34]. Other affected genes were related to RNA helicases, which regulate transcription, RNA processing, translation, and RNA replication. An important member of this family is RNA helicase A, which is a DEAD box protein, and unwinds both double-stranded DNA and RNA [35], while it binds to the pre-mRNA [36]. Since the roles of these molecules in mRNA stability and transport are not completely defined, the significance of their down-regulated expression in diabetes would be an interesting area of future investigation.

Genes relevant to various signaling molecules

Activation of PKC has been implicated in the pathogenesis of diabetic nephropathy. In our study, the genes related to mitogen- and stress-activated protein kinase (SAPK) cascades and mitogen-activated protein kinase (MAPK) pathways were also differentially expressed. The expression of mitogen- and stress-activated kinase-2 (MSK2) and MAP kinase 6c was down-regulated. MSK2 contains two catalytic domains similar to MSK1 and is activated by MAPK/ERK (extracellular signal-regulated kinase) and SAPK2/p38 kinases. In the downstream events, MSK plays a role in the activation of certain transcription factors, for example, cAMP response element-binding protein (CREB), which is induced by growth factors, cellular stresses, and various cytokines [37]. Other elements that can modulate the activity of SAPK and MAPK include nitric oxide (NO) [38], mechanical strain [39], and ceramide [40, 41], all of which have been implicated in the progression of diabetic nephropathy. With the information that the mRNA of these kinases is differentially expressed, further studies are necessary to delineate how the alterations in SAPK and MAPK pathways modulate the responsiveness to growth factors in the progression of diabetic nephropathy.

Genes relevant to extracellular matrix-related molecules

An excessive accumulation of ECM proteins, that is, types I, III, and IV collagens, fibronectin, and laminin has been well-documented in diabetic nephropathy; also, a decreased expression and sulfation of proteoglycans is implicated in the proteinuric response in diabetic nephropathy. In our experiment, the differential expression of ECM-related molecules was detected in the hypertrophic phase of diabetic STZ-induced glomerulopathy. Hyaluronic acid (HA), a glycosaminoglycan (GAG), is one of the essential components of ECM. HA-binding proteins such as CD44, aggrecan, and versican have been implicated in the assembly of ECM by stabilizing large macromolecular aggregates. Inter-α-trypsin inhibitor is also a newly identified HA-binding protein, and its H1 and H2 chains are linked in vivo and in vitro to HA. This linkage greatly improves ECM stability [42]. Fibulin-2 is another ECM protein expressed in glomeruli [43], and it has multifunctional binding activities for integrin $\alpha_{IIb}\beta_3$, fibronectin, and nidogen [44, 45]. The findings that there

is an altered expression of interalpha-trypsin inhibitor and fibulin-2 suggest that in addition to the known abnormalities in ECM in diabetic nephropathy they may also contribute to the evolution of diabetic lesions in the kidney.

Genes relevant to cell differentiation, growth, and survival

As indicated in Table 4, a differential expression of genes that modulate development, differentiation, proliferation, and apoptosis was noted during the survey by High Density Array. Interestingly, seven genes including Unc-18 homolog, POU domain transcription factor 2, lunatic fringe gene homolog, fibrous sheath component 1, Sox-17, Fibulin 2, and MRJ are involved in cell differentiation and organogenesis. However, the expression of most of these genes in the kidney is not defined, and thus, their role in the biology of kidney and the pathophysiology of diabetic kidney needs to be investigated. One may extrapolate the role of Unc-18 homolog in the in vivo renal biology, since it has been shown in cell culture systems to be involved in vesicle transport, differentiation of renal epithelia and maintenance of the polarized phenotype of certain epithelial cells [46]. Nevertheless, the findings of this investigation, indicating an altered expression in hyperglycemic state, should give some impetus to delineate further mechanisms that are involved in diabetic nephropathy and also in diabetic embryopathy that is seen in the children of women with uncontrolled juvenile diabetes.

In conclusion, the findings of this study suggest that in the early phases of diabetic nephropathy, there is a dynamic change in the expression of various genes that is related to glucose and lipid metabolism, protein synthesis and degradation, signal transduction, ion transport, and extracellular matrix. The alterations in the lipid metabolism have not been well investigated in the pathogenesis of diabetic nephropathy. However, in view of the differential expression of lipid metabolism-related genes identified in this study, it would be worth investigating how the local lipid metabolism contributes to the progression of diabetic nephropathy. In addition, investigation of the altered gene expression of intracellular protein kinase (AMPK and mitogen-and stress-activated protein kinase) would yield information about the role of these key molecules in the metabolism and cell growth and intracellular signaling in diabetic nephropathy. Also, the study of other genes with altered expression, for example, those belonging to the transcription factors and signal transduction, would yield valuable information about the processes of cell differentiation and ways organogenesis affects the early phases of diabetic nephropathy, which progresses to more severely ominous lesions like glomerulosclerosis.

Future studies should include an investigation of time-course expression and localization of these genes using isolated glomeruli and cultured mesangial and tubular cells. To achieve this purpose, the DNA microarray may be useful because only a minute amount of RNAs is needed. In addition, a functional link between the altered expression of these genes and diabetic nephropathy should be examined, since differentially expressed genes may simply reflect the response to a hyperglycemic state rather than molecular events in the progression of diabetic nephropathy.

ACKNOWLEDGMENTS

This work was supported by Uehara Memorial Foundation, The Naito Foundation, ONO Medical Foundation, Grant-in-Aid for Encouragement of Young Scientists, Ministry of Education, Science and Culture, Japan (10770199) to J. Wada; a Grant-in-Aid for Scientific Research (B), Ministry of Education, Science and Culture, Japan (11470218), Uehara Memorial Foundation to H. Makino; and a National Institutes of Health Grant DK28492 to Y.S. Kanwar. H. Zhang was supported by International Society of Nephrology/Kirin Fellowship Award. The authors thank T. Hashimoto and Y. Saito for assistance with the electron microscopy.

Reprint requests to Jun Wada, M.D., Ph.D., Department of Medicine III, Okayama University Medical School, 2-5-1 Shikata-cho, Okayama 700-8558, Japan.
E-mail: junwada@md.okayama-u.ac.jp

APPENDIX

Abbreviations used in this article are: CREB, cAMP response element-binding protein; ECM, extracellular matrix; ERK, extracellular signal-regulated kinase; EST, expressed sequence tag; GAG, glycosaminoglycan; GDA, Gene Discovery Assay; HA, hyaluronic acid; ICR, streptozotocin-induced diabetic CD-1 mouse strain; MAPK, mitogen-activated protein kinase; MSK2, mitogen and stress-activated kinase-2; NCBI, National Center for Biotechnology Information; PAM, periodic acid silver methenamine; PCR, polymerase chain reaction; PKC, protein kinase C; RDA, representational difference analysis; SAPK, stress-activated protein kinases; STZ, streptozotocin; UX, unilaterally nephrectomized.

REFERENCES

1. Wada J, Kanwar YS: Characterization of mammalian translocase of inner mitochondrial membrane (Tim44) isolated from diabetic mouse kidney. *Proc Natl Acad Sci USA* 95:144–149, 1998
2. Zhang H, Wada J, Kanwar YS, *et al:* Screening for genes upregulated in 5/6 nephrectomized mouse kidney. *Kidney Int* 56:549–558, 1999
3. Wada J, Shikata K, Makino H: Novel approaches to unravel the genesis of glomerulosclerosis by new methodologies in molecular biology and molecular genetics. *Nephrol Dial Transplant* 14:2551–2553, 1999
4. Zheng Z, Striker GE, Esposito C, Striker LJ: Strain differences rather than hyperglycemia determines the severity of glomerulosclerosis in mice. *Kidney Int* 54:1999–2007, 1998
5. Watanabe Y, Itoh Y, Yoshida F, *et al:* Unique glomerular lesion with spontaneous lipid deposition in glomerular capillary lumina in the NON strain of mice. *Nephron* 58:210–218, 1991
6. Shimizu K, Morita H, Niwa T, *et al:* Spontaneous amyloidosis in senile NSY mice. *Acta Pathol Jpn* 43:215–221, 1993
7. Makino H, Yamasaki Y, Haramoto T, *et al:* Ultrastructural changes of extracellular matrices in diabetic nephropathy revealed by high resolution scanning and immunoelectron microscopy. *Lab Invest* 68:45–55, 1993
8. Chirgwin JM, Przybyla AE, MacDonald RJ, Rutter WJ: Isola-

tion of biologically active ribonucleic acid from sources enriched in ribonuclease. *Biochemistry* 18:5294–5299, 1979
9. Wada J, Kumar A, Liu ZZ, *et al:* Cloning of mouse integrin αv cDNA and role of the αv-related matrix receptors in metanephric development. *J Cell Biol* 132:1161–1176, 1996
10. Wada J, Kanwar YS: Identification and characterization of galectin-9, a novel β-galactoside binding mammalian lectin. *J Biol Chem* 292:6078–6086, 1997
11. Wada J, Kumar A, Ota K, *et al:* Representational difference analysis of cDNA of genes expressed in embryonic kidney. *Kidney Int* 51:1629–1638, 1997
12. Takenaka M, Imai E, Kaneko T, *et al:* Isolation of genes identified in mouse renal proximal tubule by comparing different gene expression profiles. *Kidney Int* 53:562–572, 1998
13. Stumvoll M, Meyer C, Mitrakou A, *et al:* Renal glucose production and utilization: New aspects in humans. *Diabetologia* 40:749–757, 1997
14. Meyer C, Dostou JM, Gerich JE: Role of the human kidney in glucose counterregulation. *Diabetes* 48:943–948, 1999
15. Kang SS, Fears R, Noirot S, *et al:* Changes in metabolism of rat kidney and liver caused by experimental diabetes and by dietary sucrose. *Diabetologia* 22:285–288, 1982
16. Meyer C, Stumvoll M, Nadkarni V, *et al:* Abnormal renal and hepatic glucose metabolism in type 2 diabetes mellitus. *J Clin Invest* 102:619–624, 1998
17. Burcelin R, Katz EB, Charron MJ: Molecular and cellular aspects of the glucagon receptor: Role in diabetes and metabolism. *Diabetes Metab* 22:373–396, 1996
18. Hoogenberg K, Dullaart RP, Freling NJ, *et al:* Contributory roles of circulatory glucagon and growth hormone to increased renal haemodynamics in type 1 (insulin-dependent) diabetes mellitus. *Scand J Clin Lab Invest* 53:821–828, 1993
19. Winder WW, Hardie DG: AMP-activated protein kinase, a metabolic master switch: Possible roles in type 2 diabetes. *Am J Physiol* 277(1 Pt 1):E1–E10, 1999
20. Hardie DG, Carling D: The AMP-activated protein kinase: Fuel gauge of the mammalian cell? *Eur J Biochem* 246:259–273, 1997
21. Kramer-Guth A, Quaschning T, Pavenstadt H, *et al:* Uptake and metabolism of lipoproteins from patients with diabetes mellitus type II by glomerular epithelial cells. *Nephrol Dial Transplant* 12:1336–1343, 1997
22. Neverov NI, Kaysen GA, Nuccitelli R, Weiss RH: HDL causes mesangial cell mitogenesis through a tyrosine kinase-dependent receptor mechanism. *J Am Soc Nephrol* 8:1247–1256, 1997
23. Kanzaki T, Ishikawa Y, Morisaki N, *et al:* Abnormal metabolism of polyunsaturated fatty acids and phospholipids in diabetic glomeruli. *Lipids* 22:704–710, 1987
24. Belfiore F, Rabuazzo AM, Iannello S, *et al:* Anabolic response of some tissues to diabetes. *Biochem Med Metab Biol* 35:149–155, 1986
25. Cortes P, Dumler F, Goldman J, Levin NW: Relationship between renal function and metabolic alterations in early streptozocin-induced diabetes in rats. *Diabetes* 36:80–87, 1987
26. Steer KA, Sochor M, Gonzalez AM, McLean P: Regulation of pathways of glucose metabolism in kidney: Specific linking of pentose phosphate pathway activity with kidney growth in experimental diabetes and unilateral nephrectomy. *FEBS Lett* 150:494–498, 1982
27. Sochor M, Kunjara S, Baquer NZ, McLean P: Regulation of glucose metabolism in livers and kidneys of NOD mice. *Diabetes* 40:1467–1471, 1991
28. Everett RD, Meredith M, Orr A, *et al:* A novel ubiquitin-specific protease is dynamically associated with the PML nuclear domain and binds to a herpes virus regulatory protein. *EMBO J* 16:1519–1530, 1997
29. Hatzopoulos AK, Stoykova AS, Erselius JR, *et al:* Structure and expression of the mouse Oct2a and Oct2b, two differentially spliced products of the same gene. *Development* 109:349–362, 1990
30. Imataka H, Sogawa K, Yasumoto K, *et al:* Two regulatory proteins that bind to the basic transcription element (BTE), a GC box sequence in promoter region of the rat P-4501A1 gene. *EMBO J* 11:3663–3671, 1992
31. Kanai Y, Kanai-Azuma M, Noce T, *et al:* Identification of two Sox17 messenger RNA isoforms, with and without the high mobility group box region, and their differential expression in mouse spermatogenesis. *J Cell Biol* 133:667–681, 1996
32. Duncan R, Bazar L, Michelotti G, *et al:* A sequence-specific, single-strand binding protein activates the far upstream element of *c-myc* and defines a new DNA-binding motif. *Genes Dev* 8:465–480, 1994
33. Shankland SJ, Scholey JW: Expression of growth-related protooncogenes during diabetic renal hypertrophy. *Kidney Int* 47:782–788, 1995
34. Marion RM, Fortes P, Beloso A, *et al:* A human sequence homologue of Staufen is an RNA-binding protein that is associated with polysomes and localizes to the rough endoplasmic reticulum. *Mol Cell Biol* 19:2212–2219, 1999
35. Zhang S, Maacke H, Grosse F: Molecular cloning of the gene encoding nuclear DNA helicase II: A bovine homologue of human RNA helicase A and Drosophila Mle protein. *J Biol Chem* 270:16422–16427, 1995
36. Zhang S, Herrmann C, Grosse F: Pre-mRNA and mRNA binding of human nuclear DNA helicase II (RNA helicase A). *J Cell Sci* 112:1055–1064, 1999
37. Deak M, Clifton AD, Lucocq LM, Alessi DR: Mitogen- and stress-activated protein kinase-1 (MSK1) is directly activated by MAPK and SAPK2/p38, and may mediate activation of CREB. *EMBO J* 17:4426–4441, 1998
38. Huwiler A, Pfeilschifter J: Nitric oxide stimulates the stress-activated protein kinase p38 in rat renal mesangial cells. *J Exp Biol* 202:655–660, 1999
39. Ingram AJ, Ly H, Thai K, *et al:* Activation of mesangial cell signaling cascades in response to mechanical strain. *Kidney Int* 55: 476–485, 1999
40. Coroneos E, Wang Y, Panuska JR, *et al:* Sphingolipid metabolites differentially regulate extracellular signal-regulated kinase and stress-activated protein kinase cascades. *Biochem J* 316:13–17, 1996
41. Zador IZ, Deshmukh GD, Kunkel R, *et al:* A role for glycosphingolipid accumulation in the renal hypertrophy of streptozotocin-induced diabetes mellitus. *J Clin Invest* 91:797–803, 1993
42. Bost F, Diarra-Mehrpour M, Martin JP: Inter-alpha-trypsin inhibitor proteoglycan family: A group of proteins binding and stabilizing the extracellular matrix. *Eur J Biochem* 252:339–346, 1998
43. Reinhardt DP, Sasaki T, Dzamba BJ, *et al:* Fibrillin-1 and fibulin-2 interact and are colocalized in some tissues. *J Biol Chem* 271:19489–19496, 1996
44. Pfaff M, Sasaki T, Tangemann K, *et al:* Integrin-binding and cell-adhesion studies of fibulin reveal a particular affinity for αIIbβ3. *Exp Cell Res* 219:87–92, 1995
45. Sasaki T, Gohring W, Pan TC, *et al:* Binding of mouse and human fibulin-2 to extracellular matrix ligands. *J Mol Biol* 254:892–899, 1995
46. Lehtonen S, Riento K, Olkkonen VM, Lehtonen E: Syntaxin 3 and Munc-18-2 in epithelial cells during kidney development. *Kidney Int* 56:815–826, 1999